DESIGN AND ANALYSIS OF CORIOLIS MASS FLOWMETERS USING MSC/NASTRAN

C. P. Stack and T. J. Cunningham
7070 Winchester Circle
Micro Motion, Inc.
Boulder, Colorado

Abstract

A Coriolis mass flowmeter measures mass flow directly by vibrating a fluid-conveying pipe at resonance. Design of these meters was facilitated by solving the equations of motion via the finite element method. A complex eigenvalue analysis (SOL107) was necessary due to the presence of the Coriolis force terms in the damping matrix. Performance parameters of the meter can be predicted from the complex eigenvectors and were found to match experimentally determined values to within five percent

Since vibration occurs during Coriolis meter operation, low stress designs must be used to preclude fatigue failure. This analysis was also performed using MSC/NASTRAN

I. Introduction

Process industries usually require precise measurement of mass flow rate. A conventional flow metering system such as a turbine meter measures volumetric flow and calculates mass flow rate indirectly. Volumetric flow can be corrected to mass flow rate if the precise fluid density is known. However, changes in a fluid's temperature, pressure, viscosity, and composition can all affect the fluid density, reducing the accuracy of indirect mass flow rate calculations.

A Coriolis mass flowmeter directly measures the mass flow rate of a fluid by vibrating (driving) a fluid-conveying pipe at resonance. The directional change in the moving fluid due to the pipe vibration develops Coriolis forces. The Coriolis forces act on the pipe to perturb the vibrational motion, giving rise to a spatially varying phase angle along the pipe. The mass flow rate of a Coriolis sensor is directly proportional to the phase delay between any two points on the pipe.

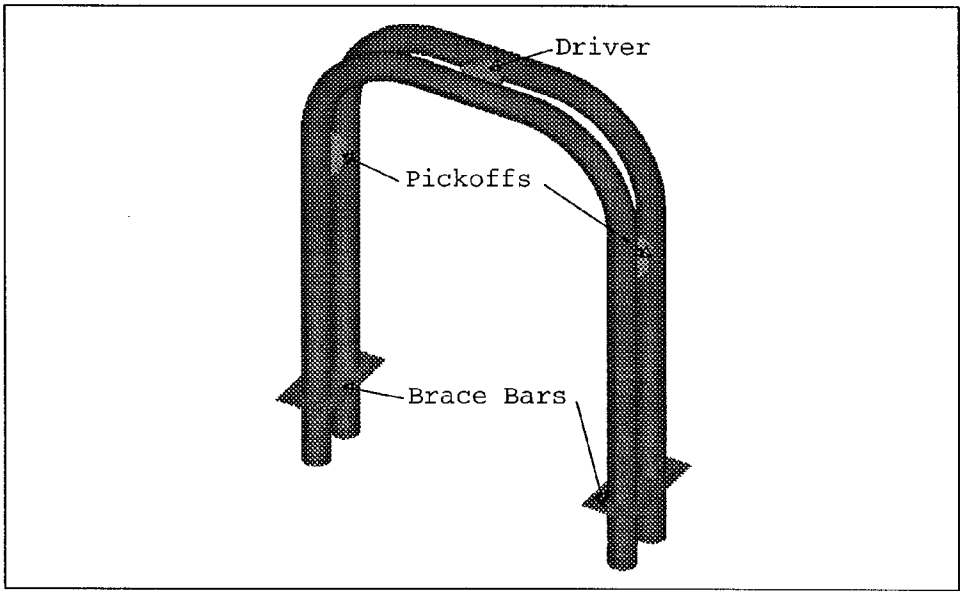

Figure 1 Typical Coriolis Flowmeter

The two points where phase angles are measured, labeled "Pick-offs" in Figure 1, are instrumented, typically, with velocity detectors. It is common practice to get the phase difference via a measurement of the time delay, Δt, between zero crossings of these velocity signals.

The phase angle, $\Delta\theta$, can be related to this time delay by

$$\Delta t = \Delta\theta/\omega \tag{1}$$

where $\Delta\theta$ is the phase delay and ω is the driving frequency. Mass flow rate is proportional to time delay by

$$\dot{m} = \kappa \Delta t \tag{2}$$

The proportionality constant, κ, is called the calibration factor and is a measure of how sensitive a sensor is to mass flow rate.

Several researchers have developed analytical methods to predict the behavior Coriolis mass flowmeters [1,2]. These methods are limited to simple geometry and boundary conditions. The finite element method was used to predict the behavior of Coriolis mass flowmeters [3]. MSC/NASTRAN was used in the implementation of the finite element method, as well as being used for the prediction operating stresses in the meter.

II. Problem Definition

The design of a new Coriolis mass flowmeter starts with identifying a new application. A flow chart of the design cycle is shown in Figure 2. Marketing research defines this application in terms of the maximum mass flow rate, the maximum allowable pressure drop, and the type of fluid that will be measured.

The sensor design engineer translates the market definition into design specifications. The primary design specification, the target calibration factor, follows directly from the maximum flow rate. Sensor electronics require a certain time delay at the sensor's maximum flow rate. This time delay and the maximum flow rate are entered into Equation (2), which specifies the target calibration factor.

The engineer also generates additional design specifications. The second design specification involves the dynamic behavior; i.e. the natural frequencies and eigenvectors (mode shapes). Micro Motion, based on years of experience in Coriolis sensor design and manufacture, has developed guidelines for the natural frequencies of the sensors. These guidelines require that none of the first few natural frequencies be an integral multiple of the drive frequency. The drive frequency is the frequency at which the pipe is vibrated during normal operation. Additionally, these frequencies should not be an integral multiple of 50 or 60 *Hz*. All of the associated modes shapes need to be well understood, particularly their impact on introducing extraneous motion into the pickoffs.

The third design specification limits the level of operating stress. The sensor is subjected to bending stress due to the vibration of the pipe. Bending stress must be well below the endurance limit of the pipe material. The pipe is also stressed due to fluid pressure. The pipe wall must be thick enough to keep the pressure stress below guidelines established by ASME piping codes.

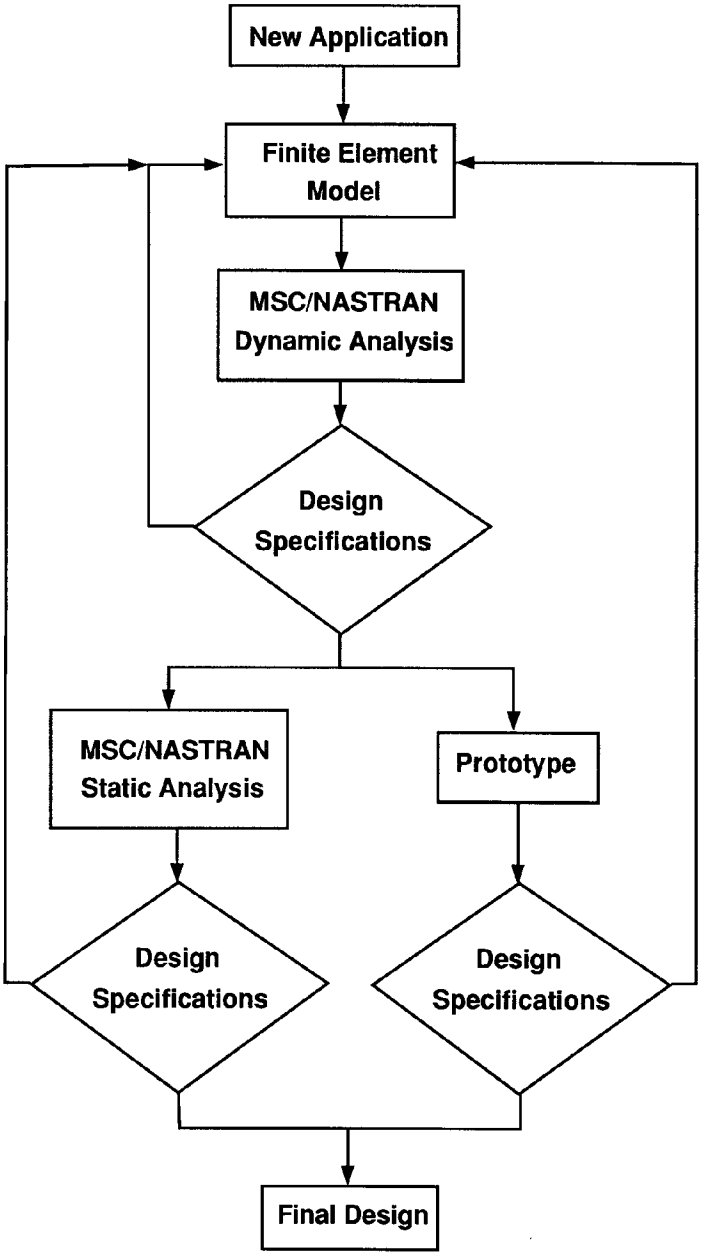

Figure 2 Design cycle flow chart

Additionally, the operating stress, which is a superposition of the bending stress and pressure stress, must be below design limits.

After compiling these design specifications, the engineer uses the marketing requirement for

pressure drop and fluid type to develop the finite element model. The allowable pressure drop at the maximum flow rate determines the size of the pipe. The type of fluid service determines what material is used for the pipe. The engineer creates a finite element model using the pipe geometry and the material properties. MSC/NASTRAN is used to analyze the FE model to predict the calibration factor, the natural frequencies and mode shapes, and the operating stress.

The designer then compares the predicted calibration factor against the design specification. If it doesn't match, the designer starts a new iteration. The relationship between the calibration factor and the pressure drop as a function of the pipe properties is not straightforward. For example, a long thin flexible pipe will have a small calibration factor; i.e. will have a large time delay for a small flow, but will have a large pressure drop. The designer's goal is to design a flow pipe with less than the allowable pressure drop that has the specified calibration factor. Many iterations are required to arrive at this optimum meter design.

At each iteration the engineer also has to review the model against the other design specifications. The dynamic behavior is analyzed by reviewing the frequencies and mode shapes predicted by MSC/NASTRAN against the design guidelines. The operating stress from the drive mode can be quickly checked by scaling the beam stresses from the appropriate eigenvector. Even though the actual operating stress is much more complex, the beam stress check provides immediate feedback to keep the design iterations on the right track for a viable design.

With a software model a design can be prototyped and analyzed in a matter of hours. Perhaps a dozen iterations are required to develop a design that meet all of the specifications. A hardware prototype is then built. The prototype is flow tested to confirm the predicted calibration factor. The predicted natural frequencies are compared to experimentally measured frequencies. These two tests provide a check for the validity of the model.

In parallel with the prototype testing, the operating stress is analyzed using MSC/NASTRAN. A dual pipe sensor incorporates brace bars (see Figure 1) to separate the natural frequencies. Operating stresses are highest adjacent to the brace bar, requiring a detailed finite element model for an accurate representation of the stress field.

It is clear that design iterations performed in software are crucial to the sensor design cycle. Key to the software model are the several analyses performed by MSC/NASTRAN.

III. Analysis

Finite element analysis (FEA) done in support of the design cycle can be divided into two basic types. Dynamic analysis was performed using MSC/NASTRAN's complex eigensolver and a custom fluid-elastic beam element, and stress analysis was performed using standard elements

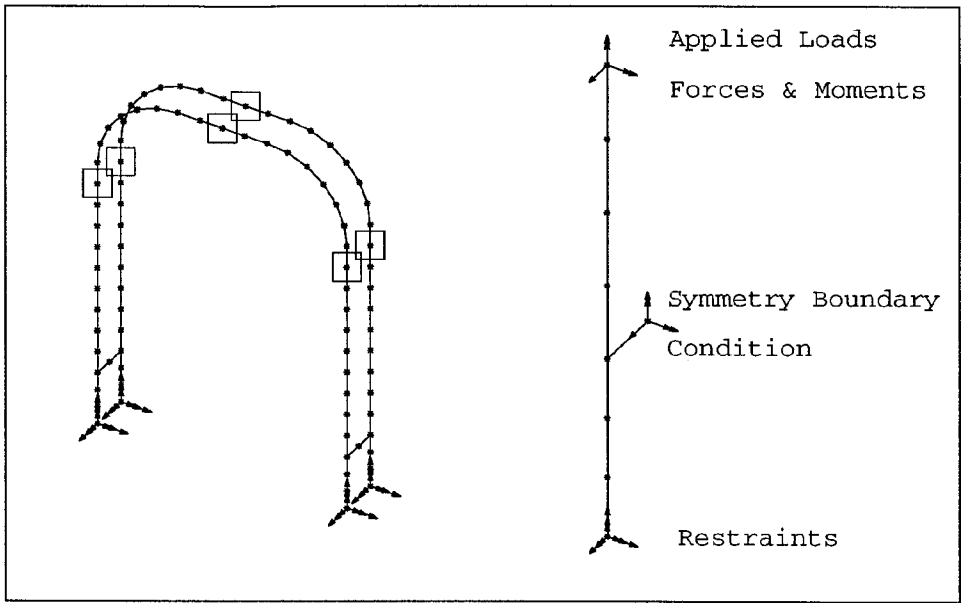

Figure 3 Beam model used for dynamic analysis (left), beam model used for static analysis (right)

from the MSC/NASTRAN element library. These two types of analyses will be discussed separately.

Dynamic Analysis Dynamic analysis is performed early in the design cycle to estimate meter parameters such as calibration factor, natural frequencies and mode shapes. These parameters are predicted using FEA, where the finite element model is shown in Figure 3, and a custom beam finite element. This custom beam element was formulated to account for the fluid-structure interaction of the fluid-conveying pipe[3]. The formulation of this element will not be discussed in detail. However, the manner in which it was incorporated into MSC/NASTRAN will be reviewed.

The equations of motion for the fluid-conveying beam were expressed in finite element notation as,

$$[\mathbf{M}]\frac{d^2\mathbf{q}}{dt^2} + [\mathbf{B}]\frac{d\mathbf{q}}{dt} + [\mathbf{K} - \mathbf{C}]\mathbf{q} = 0 \tag{3}$$

where [M], [B], and [K – C] are the mass, Coriolis and stiffness matrices, respectively, and q is the vector of time dependant nodal values. While Equation (3) is the standard finite element expression for a complex eigenvalue problem, the components of the matrices differ from the typical finite element formulation. The origin of this difference is the modelling of the fluid-structure interaction.

Each of the matrices of Equation (3) are composed of several different terms. The mass matrix has contributions from the mass of the pipe and the mass of the fluid, and can be expressed as,

$$[M] = [M_p] + [M_f] \tag{4}$$

where the subscripts p and f denotes pipe and fluid, respectively.

The [**B**] matrix, in the absence of structural or material damping, is composed entirely of terms arising from the Coriolis effect and is asymmetric. Unlike damping, the Coriolis effect, in general, does not result in decaying free vibrations.

The final matrix, stiffness, is composed of terms arising from the stiffness of the pipe and from centrifugal acceleration. This matrix can be expressed as,

$$[K - C] = [K_p] - [C_f] \tag{5}$$

where $[K_p]$ represents stiffness of the pipe and $[C_f]$ denotes the centrifugal acceleration of the fluid.

The various components of the matrices ($[M_p]$, $[M_f]$, $[B]$, $[K_p]$ and $[C_f]$) were imported into MSC/NASTRAN via DMIG (Direct Matrix Input at Grid points) entries. The linear algebra capabilities of DMAP (Direct Matrix Abstraction Program) were then used to assemble the matrices of Equation (3). Using this methodology has several advantages specific to the design of Coriolis mass flowmeter.

Coriolis mass flowmeters typically are used over a range of mass flow rates and fluid densities, and hence it is important to investigate meter dynamics over these ranges. Three of the component matrices ($[M_f]$, $[B]$, and $[C_f]$) are functions of fluid density, mass flow rate, or both. The DMIG entries of these matrices were therefore normalized to unit fluid density (fluid density is set Equal to one) and unit mass flow rate, and then written to a data file along with the mass and stiffness matrices of the pipe. Multiple MSC/NASTRAN data decks were then created which included this data file and scaled the matrices, via DMAP, to the appropriate fluid density and mass flow rate values prior to their assembly in Equation (3). This entire process, from the creation of the file containing the DMIG entries to the creation of multiple data decks, was contained within a single FORTRAN program. Thus, by answering a few simple prompts issued by the FORTRAN program, the engineer was allowed to analyze a proposed meter design over a wide range of fluid densities and mass flow rates.

Although the matrices were not standard, standard MSC/NASTRAN solvers could be used. This was because the equations of motion, Equation (3), were in standard form and because of MSC/NASTRAN's ability to handle asymmetric matrices.

The solution sequence used in the prediction of calibration factors, natural frequencies, and eigenvectors was SOL107, the structured solution sequence for a complex eigenvalue analysis.

Output from this solution sequence consisted of the complex eigenvalues from which natural frequencies were readily available, and mode shapes which were used in the determination of the calibration factor. Mode shapes were written to the f06 file in magnitude and phase angle format to facilitate the calibration factor calculation.

Calculation of the calibration factor was achieved by post-processing the mode shapes. Equation (1) was used to convert the difference in phase angle to a time delay between any pair of nodes, where the node pair represents possible velocity detector locations. This conversion was performed for the mode shape chosen to represent the drive mode. Time delay can then be converted to a calibration factor via Equation (2). Thus, for any single analysis, the post processor can be run any number of times to investigate various velocity detector locations or to select different mode shapes as the drive mode.

Although the primary function of Coriolis meters is the determination of mass flow rate, they can also be used to measure process fluid density. This is done by correlating the change in drive frequency with the change in fluid density. The correlation between drive frequency and fluid density is done by measuring (calibrating) drive frequency on two known fluids, typically air and water, at zero fluid velocity. The density of the fluid is then estimated through interpolation using the known frequencies. This density measurement process can be simulated analytically by analyzing the meter at several different fluid densities. (Note: In actual practice drive period is monitored instead of drive frequency. Since period is simply the reciprocal of frequency, the discussions of this section are applicable.)

The procedure described above is used by the designer to iterate on potential meter designs. Once a design has been found that meets all of the performance criterion, such as calibration factor, a prototype is built to verify the design. At this point a detailed stress analysis is also performed.

Stress Analysis Stress analysis is performed at several different stages of the design cycle. The first stress analysis occurs early in the design cycle when the dynamics of the meter are being investigated. Utilizing the beam model used for the fluid-elastic analysis of the previous section, Figure 3, the engineer performs a second eigenvalue analysis. The custom beam elements are replaced with CBAR elements, while the mass of the pick-offs and driver are modeled with CONM2 elements. The output requested from this analysis includes beam stresses, along with eigenvectors. The analysis results are scaled such that the displacements of the eigenvector match the displacements anticipated by the designer. This stress analysis is used as a sanity check, and is replaced with a more rigorous stress analysis once a meter design is finalized.

Upon finalization of a meter design, detailed stress analyses of the pipe-to-brace bar joint (braze joint) under operational loading are performed using the model shown in Figure 4. Operational loading consists of internal pressure and vibration-induced bending. Both of these analyses are linear-elastic static analyses and utilized solid continuum elements to model the braze joint. The

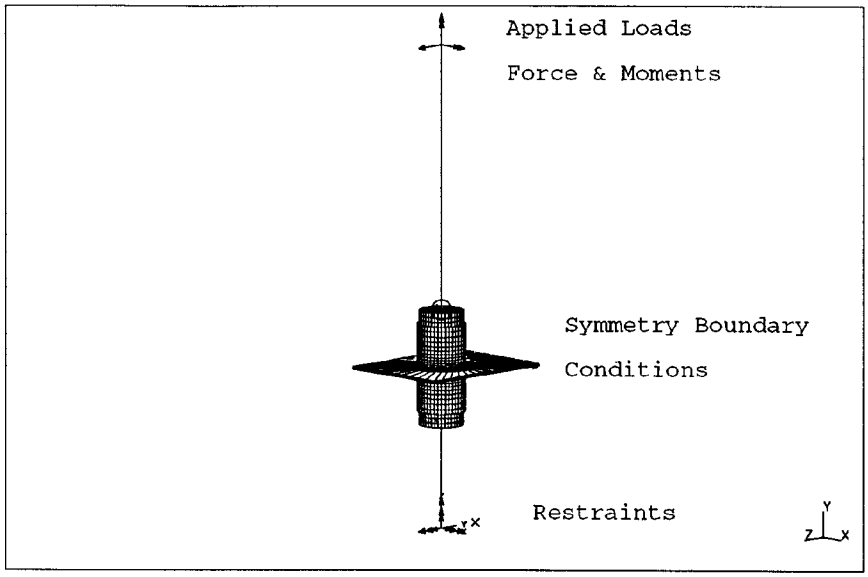

Figure 4 Detailed model of the braze joint

solid continuum elements near the braze joint allowed for accurate prediction of the stress field in this region. Away from the braze joint, the solid continuum elements make a transition to shell elements, which then make a transition to beam elements. The modeling procedure used in these transition regions were described in Reference [4].

The internal pressure load was relatively easy to simulate. All of the internal free-faces of the model were loaded with a face pressure equal to the maximum operating pressure. Also an axial load was applied to the node labeled "applied loads" in the Figure simulating the axial straining caused by the bent-pipe design.

Estimation of the stress arising from vibration required several finite element analyses. The analyses were linked together such that the output of one analysis was used as the input for the subsequent analysis. The first analysis performed was a real eigenvalue, or normal modes, analysis. This analysis was a repeat of the stress analysis performed in support of the dynamic investigation, except that the results requested consisted of internal forces and moments in addition to mode shapes. The results corresponding to the drive mode were scaled such that the displacements of a pick-off node predicted by the eigenvector matched the actual displacement measured from a hardware prototype. These scaled forces and moments were then used in subsequent analyses.

The first of two linear-elastic static analyses was performed using beam elements. The beam model employed was a subset of the original beam model used for the normal modes analysis,

see Figure 3. Boundary conditions applied to this model simulated the symmetry of the meter and also simulated the forces and moments arising from vibration. The displacements predicted by this model were compared to the eigenvector displacements. This was done to ensure that the loads were applied correctly.

The final analysis performed was a linear-elastic static analysis which used the model shown in Figure 4. The loads and boundary conditions applied to the beam model were also applied to this model as shown in the Figure. The result of this analysis is an accurate representation of the stress field arising from the vibration-induced bending.

The stress field arising from operational loading, internal pressure and bending, was then created by superposition of the result from the detailed analyses already discussed. These stresses were then compared to design limits to assess the integrity of the design.

IV. Results and Discussion

Fluid-Elastic Analysis Solution of the equations of motion via SOL107 yields a set of complex eigenvalues and their corresponding mode shapes. Figure 5 shows the deformed geometry plot of the real and imaginary components of the mode shape in which the meter of Figure 1 is driven. Alternatively, the real and imaginary components of a mode shape may be combined into a single deformed geometry plot. Figure 6 shows this deformed geometry plot, along with the same mode under the condition of no fluid flow.

Combining the real and imaginary components of a mode into a single deformed geometry plot shows the spatially varying phase angle caused by fluid flow. This phase angle perturbs the no flow mode shape. This perturbation of the mode shape is evident in Figure 6. The amount of the induced perturbation is proportional to mass flow rate and allows Coriolis mass flowmeters to measure mass flow rate directly.

The mode of operation of a meter is a design choice. All modes are perturbed by the presence of flowing fluid, and hence mass flow rate measurements could be made if the meter were driven in any other mode. Thus the discussion and results presented here are applicable to all Coriolis meters, and are not restricted to those driven in the mode illustrated by Figures (5 and 6).

Calibration factors were predicted by post-processing the phase information of the mode shapes contained in the f06 file. These calibration factors were found to match experimentally determined calibration factors to within five percent for a variety of meter designs[3]. The influence of process fluid density on calibration factor was investigated by performing the fluid-elastic analysis over a range of densities. Figure 7 illustrates the results of this analysis. The engineer can use this information to minimize the influence of process fluid density on calibration factor.

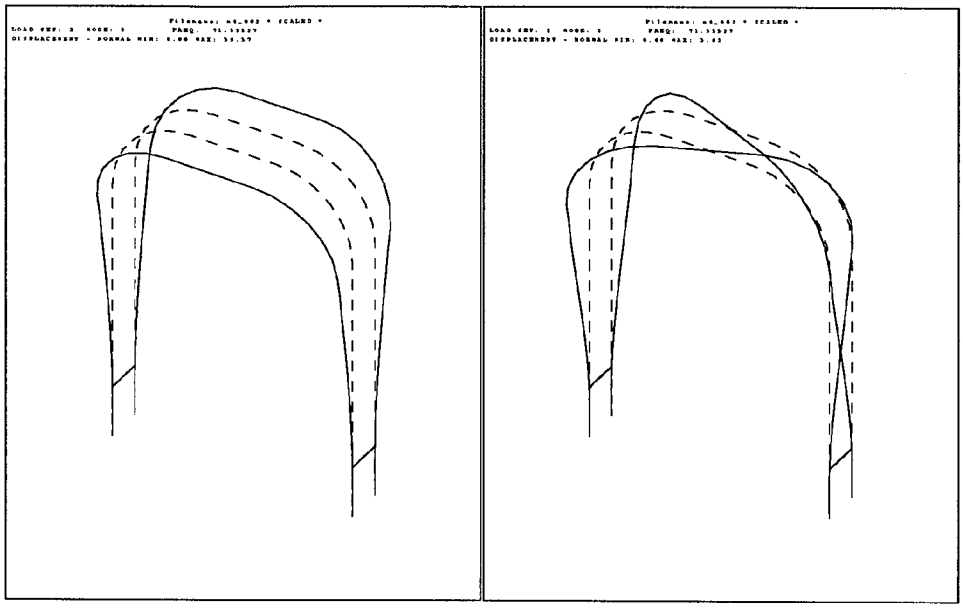

Figure 5 Deformed geometry of the real (left) and imaginary (right) components of an eigenvector

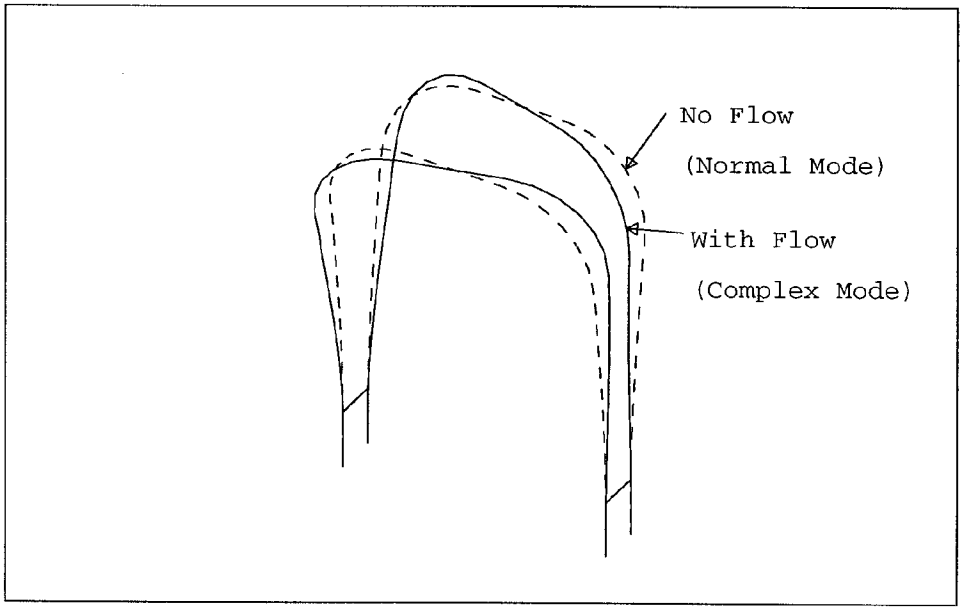

Figure 6 Eigenvectors under fluid flowing and no fluid flow conditions

Another aspect of meter dynamics that is crucial to meter performance is the distribution of eigenvalues. Eigenvalues should not lie on integer multiples of 50 or 60 *Hz* or lie on an integer multiple of the drive frequency. The first restriction limits the influence that external sources,

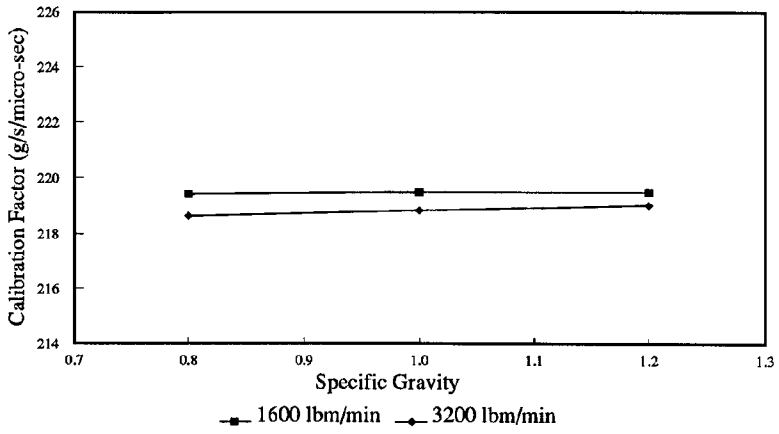

Figure 7 Density effects on calibration factor

such as pumps, can have on the dynamics of the system. The second restriction is imposed to reduce the influence that modes, other than drive, can have on the velocity signal generated by the pick-offs. Compliance to these limits is assured by reviewing the natural frequencies predicted by the complex eigenvalue analysis. Table 1 lists the first six eigenvalues computed for the meter of Figure 1 on air and water. The values listed correspond to the no-flow condition, but can be easily generated over the entire flow range of the meter.

Mode Number	Predicted Natural Frequency	
	Air (*Hz*)	Water (*Hz*)
1	72.9	60.8
2	85.8	71.6
3	126	105
4	140	117
5	191	159
6	221	184

Table 1 Predicted Meter frequencies on air and water

Mode 1 of Table 1 appears to be in direct violation of the above stated rules. This mode, however, is highly dependent upon the boundary conditions and other effects, such as the presence of manifolds and cases which were not modeled by the finite element analysis. Experimental modal analysis is therefore performed to check the predicted natural frequencies.

Figure 8 shows the change in predicted drive frequency versus mass flow rate for fluid of various specific gravities. Figure 8 clearly indicates that mass flow rate also influences drive frequency.

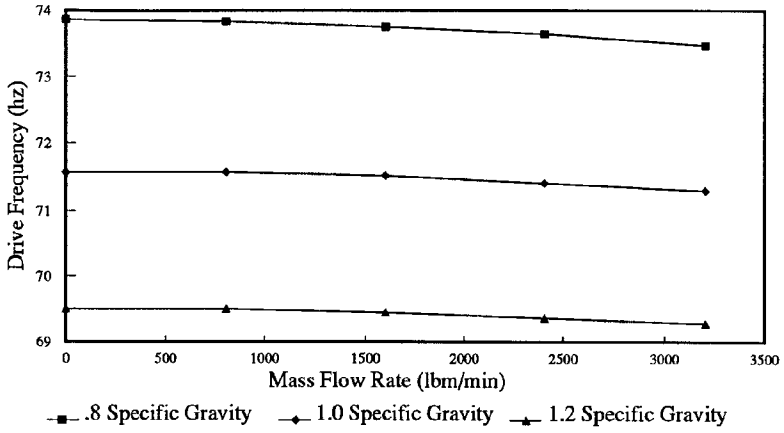

Figure 8 Predicted drive frequency versus mass flow rate for various densities

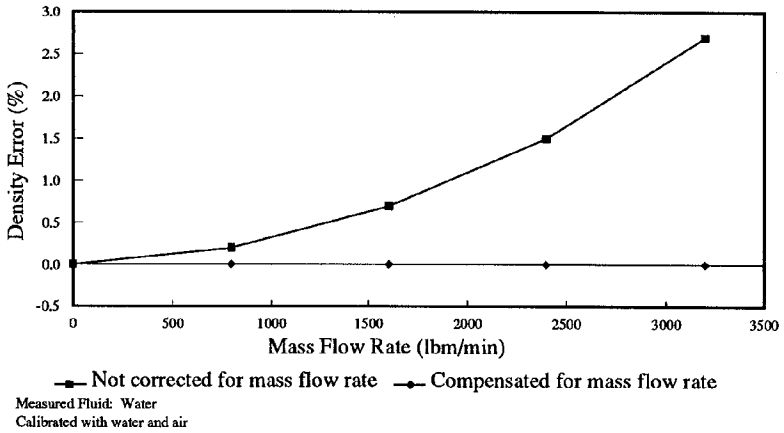

Figure 9 Error in density prediction versus mass flow rate

Thus, prediction of fluid density by assuming that the change in drive frequency is strictly a function of fluid density is incorrect. Micro Motion, Inc. has developed a technique for correcting the influence of mass flow rate on density predictions[5]. This technique requires the use of a third density calibration point generated at a known mass flow rate and process fluid density. Figure 9 illustrates the improvement in density prediction when corrected for mass flow rate.

Stress Analysis Results of the stress analysis done in support of the dynamic investigation are shown in Figure 10. The ordinate in the Figure represents the spacing between nodes starting at the pipe inlet and proceeding to the outlet. The abscissa of the figure is the bending stress scaled in the manner previously discussed. The points of maximum bending stress occur at the nodes representing the braze joints, indicating the need for a detailed analysis of this region. Only one pipe was represented in the figure. A plot of the other pipe would be identical because of symmetry.

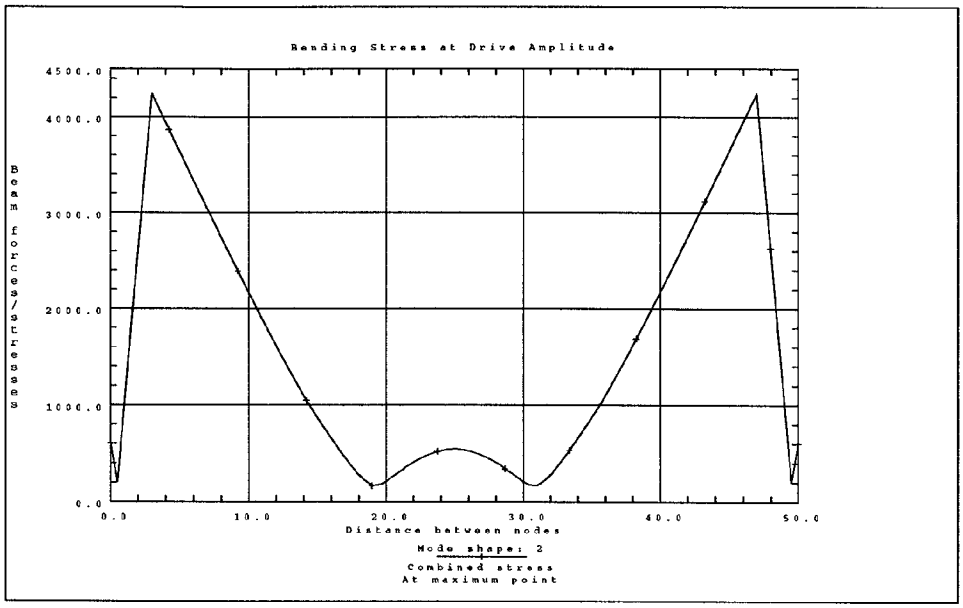

Figure 10 Beam stress calculated from a normal modes analysis

Several static analyses were used to estimate the stress caused by vibration-induced bending. The first static analysis was performed using a simple beam model. The displacements and rotations from this model were used to verify the loading applied to the detailed stress model. Table 2 shows this comparison.

Model Type	Displacement and Rotations			External Work ($lbf \cdot in$)
	D_z (in)	R_x (rad)	R_y (rad)	
Beam	-1.99E-3	9.84E-4	3.48E-5	0.200
3-D	-1.97E-3	9.81E-4	3.65E-5	0.199

Table 2 Verification of the bend load

After the loading has been verified, stresses predicted from the detailed model are analyzed. Figure 11 shows the bending stresses. The magnitude of the bending stresses of this model were above those predicted by the beam model and were found to be dependent upon such variables as pipe wall thickness, brace bar thickness, braze fillet radius, etc. Thus the detailed model is necessary to accurately predict the stresses in this region.

Results from the analysis of internal pressure are shown in Figure 12. The stress field and displacement field are clearly influenced by the braze joint. Away from the braze joint the stresses conform to those predicted analytically; i.e. Lame's solution.

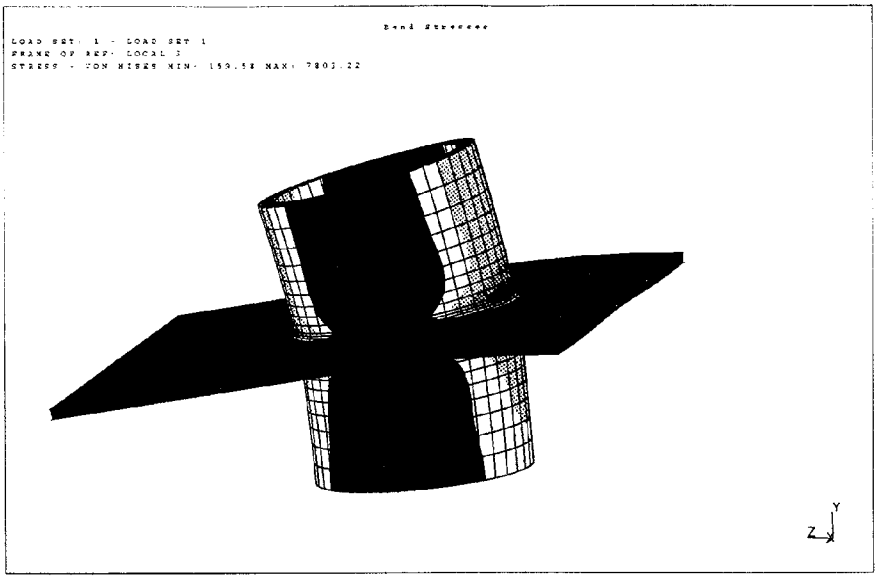

Figure 11 Von Mises stress arising from bending

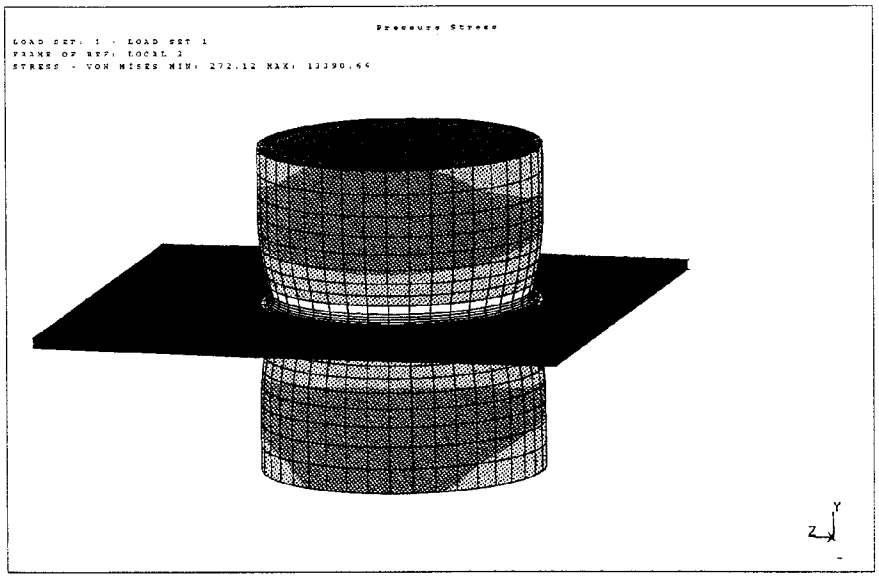

Figure 12 Von Mises stress arising from internal pressure

Operational stress is the combination of the two stress states already discussed, and was formed by superposition. Figure 13 displays this combined stress state. Once again, Figure 13 illustrates

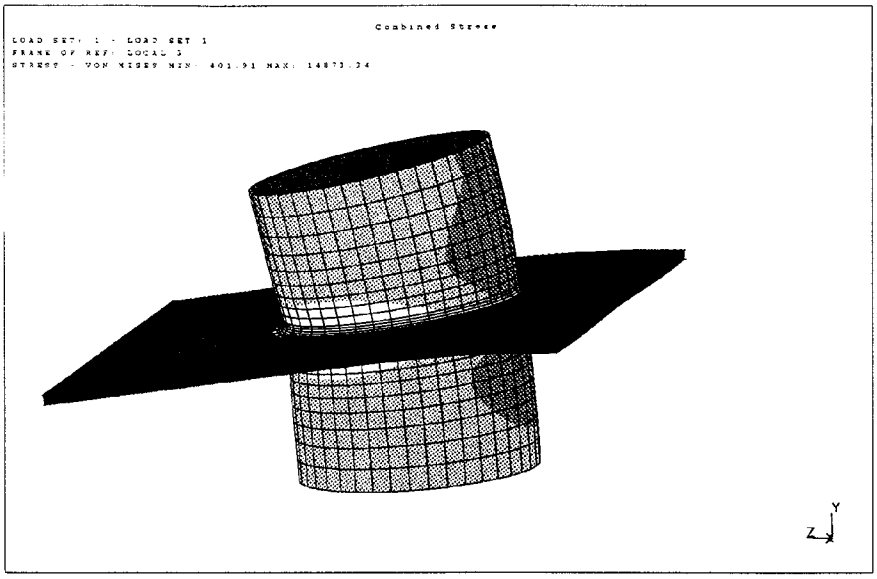

Figure 13 Von Mises stress arising from meter operation

the complexity of the stress field near the braze joint. Operational stresses are used to compare to design limits. Design limits were chosen to preclude fatigue failure.

V. Conclusions

MSC/NASTRAN is used extensively in the design and analysis of Coriolis mass flowmeters. The early portion of the design cycle focuses on the prediction of meter dynamics. MSC/NASTRAN was used at this stage to solve (SOL107) the equations of motion of a custom beam finite element. This finite element was imported into MSC/NASTRAN via DMIG entries. Additionally the linear algebra capabilities of DMAP were used to allow the engineer to analyze an entire spectrum of mass flow rates and fluid process densities with a single finite element model.

Standard MSC/NASTRAN elements and solutions were also used at various points in the design cycle to estimate stress. Estimation of stress is necessary to preclude fatigue failure. The ability to predict both meter dynamics and stress in software significantly shortens the development time for new Coriolis mass flowmeters.

VI. Acknowledgments

The authors of this paper would like express gratitude to Mr. Rob Garnett for all the work he has done programming the interface to MSC/NASTRAN and also to Mr. Mark Miller, of MSC,

for the work he performed in developing the solution methodology used to analyze Coriolis mass flowmeters for stress.

References

[1] J. D. Titlow. A Fluidelastic Analysis of Coriolis Mass Flowmeters. *In preparation*, 1993.

[2] H. Raszillier and F. Durst. Coriolis-effect in Mass Flow Metering. *Archive of Applied Mechanics*, 61(3):192–214, 1991.

[3] C.P. Stack, R.B. Garnett, and G.E. Pawlas. A Finite Element fot the Vibration Analysis of a Fluid-Conveying Timoshenko Beam. In *The 34th SDM Conference, May 1993*, La Jolla, CA. AIAA.

[4] D. S. McCollum. Using the CQUAD4 Element to Model the Interface Between Solid and Shell Finite Elements. In *The MSC 1991 World Users' Conference Proceedings, Vol II, Paper 58*, 1991.

[5] J. D. Titlow, D. S. McCollum, P. Aranuchalam, and B. Bruck. Vibrating Tube Densimeter. *Patent Applied for October 1992.*